Nuclear Instruments and Methods in Physics Research A ▮ (▮▮▮▮) ▮▮▮–▮▮▮

Contents lists available at ScienceDirect

Nuclear Instruments and Methods in Physics Research A

journal homepage: www.elsevier.com/locate/nima

Progress in X-ray imaging and spectroscopy of ultraintense laser matter interactions

L.A. Gizzi [a,b,*], P. Köster [a,b], L. Labate [a,b], T. Levato [a,c]

[a] ILIL, INO-CNR Sez. Pisa, CNR Campus, Via G. Moruzzi, 1-Pisa, Italy
[b] INFN, Sez. di Pisa, Largo B. Pontecorvo 3, Pisa, Italy
[c] FLAME, LNF, INFN, Frascati, Italy

ARTICLE INFO

Keywords:
Ultra-intense laser-matter interactions
X-ray spectroscopy
X-ray imaging
Fast electron transport
Single photon detection

ABSTRACT

Energetics of ultraintense laser-matter interactions are strongly characterized by production of large currents of high energy electrons. We describe recent progress in diagnostics of such electrons and related processes. We use an Energy Encoded Pin-Hole Camera, a novel X-ray imaging technique based on single photon detection to investigate generation and transport of such high energy electrons following the interaction of femtosecond laser pulses with solids at intensities exceeding 5×10^{19} W/cm^2. The imaging system was configured to work in a single-photon detection regime to identify the energy of the X-ray photons and to discriminate among different X-ray emission processes.

1. Introduction

The development of chirped pulse amplification (CPA) lasers [1,2] has opened a new interaction regime characterized by ultrashort and ultraintense laser pulses and steep density gradient plasmas [3]. Recently, most of the applications of laser–plasmas rely on the efficient production of energetic electrons driven by the interaction of ultraintense laser pulses with plasmas created from solids or gases. In fact, in these interaction conditions, laser energy is efficiently transferred to electrons generating a population of so-called fast or hot electrons.

Generation and transport of fast electrons driven by ultraintense laser pulses are the key to inertial confinement fusion (ICF) in the fast ignition (FI) approach [4]. In view of this, a large effort is ongoing at large and smaller scale high-power laser laboratories to develop experimental techniques applicable to fast-ignition relevant experiments and planned future full scale installations like the European High Power Laser Energy Research facility (HiPER) [5]. Fast electrons also provide the basic mechanism for emission of Kα ultrashort X-ray pulses [6–8]. Moreover, fast electrons play a crucial role in laser driven ion acceleration [9] that has gained considerable attention because of the extremely diversified potential applications.

In all these experiments fast electron currents are well above the Alfven limit [10], and therefore transport strongly depends upon the conductivity of the medium [11] which must support propagation by supplying a balancing cold electron return current. Understanding of these phenomena requires accurate measurements, mainly based upon imaging and spectroscopy in the X-ray domain. The process of fast electron generation mainly takes place near the critical density (the density at which the laser frequency ω_0 equals the local plasma frequency ω_{pe}) surface [12,13] due to resonance absorption or vacuum heating [14], but may also arise from collisionless damping of electron plasma waves generated in the underdense plasma by laser-driven instabilities. Measurements of the angular distribution of fast electrons can be used to trace back the process and identify the originating mechanism as discussed in Ref. [15]. These hot electrons, with energies ranging from some tens of keV up to the MeV range, can penetrate the underlying cold target material, leading to inner shell ionization of the target atoms. Successive de-excitation of the ionized atoms through radiative transitions leads to the emission of characteristic K shell lines, in particular the Kα line. As the production of energetic electrons only occurs during the laser pulse, in principle, Kα sources with sub-picosecond pulse duration can be achieved [16]. Extensive experimental studies on Kα sources were reported by several groups, regarding X-ray yield measurements [17,18], polarization dependent laser absorption studies [19,20], spatial [21,22], temporal [23] characterization of the X-ray emission and the effect of prepulses on the X-ray conversion efficiency [6,24].

Here we describe an experimental investigation of fast electron transport in solids irradiated at relativistic laser intensities. Basic diagnostic techniques are briefly presented along with their limitations, followed by an introduction of single-hit spectroscopy. Techniques based upon space-resolved spectroscopy are introduced in view of their application to both ultrashort Kα X-ray sources and fast ignition studies. Spectroscopy based upon single-photon detection is unveiled as a

* Corresponding author at: ILIL, INO-CNR Sez. Pisa, CNR Campus, Via G. Moruzzi, 1-56124-Pisa, Italy
E-mail address: la.gizzi@ino.it (L.A. Gizzi).

0168-9002/$ - see front matter © 2010 Published by Elsevier B.V.
doi:10.1016/j.nima.2010.04.145

complementary technique to well established bent crystal spectroscopy. Application of this technique to the study of X-ray fluorescence emission from fast electron propagation in multi-layer targets is reported and explored as an example case.

2. Basic spectroscopy techniques

Fast electron transport is mainly being investigated in experiments in which fast electrons, with energies ranging from some tens of keV up to the MeV range, generated by the laser interaction at the target surface, penetrate the underlying cold target material, leading to X-ray emission through fluorescence, the so-called Kα emission via inner shell ionization of the target atoms. As a consequence, Kα emission can be considered as a fundamental diagnostics for these electrons [25,26]. The basic mechanism behind this process is the dependence of the fluorescence yield upon the energy of the electrons.

As an example, in Titanium, the cross-section [27] has a pronounced peak between 10 and 100 keV. Above this value, the cross-section decreases rapidly, reaching a minimum around 1 MeV and increases logarithmically for relativistic energies. Similar behaviour is found for different materials making it possible to estimate the expected response of each target material to a given energy of the fast electrons. Additionally, complementary information on the transport of fast electrons may be inferred from the X-ray Bremsstrahlung emission from the fast electrons undergoing collisions in the material or deflection due to the strong, self-generated magnetic fields as discussed in Ref. [28].

From an experimental viewpoint, several techniques are traditionally employed depending upon the required spectral and spatial resolution. Recently, schemes based upon grazing incidence optics have been successfully employed for microscopy of laser–plasmas in relatively soft X-ray range [29]. Bent Bragg crystals coupled either to X-ray films or to CCD detectors are among the mostly used X-ray diagnostics for spectroscopy of laser-produced plasma X-ray emission. Configurations with spherical crystals have been successfully used now for several years for fluorescence emission in fast electron transport experiments [30]. While allowing micrometer-scale spatial resolution to be achieved, bent crystals in the Bragg configuration suffer from some important limitations. In general, their use in relativistic laser–plasma interaction environments is made difficult by noise issues [31], especially in those configurations requiring short distances between source, crystal and detector. Another important limitation is the small range of Bragg angles typically available in configurations for 2D monochromatic X-ray imaging. This is of a key importance when dealing with fluorescence emission from fast electrons in solids. In fact, the material from which Kα originates may undergo heating and subsequent ionization that can result in a spectral blue shift of the observed Kα line due to the reduced screening effect of the nuclear charge by the outer electrons due to ionization. This effect may result in a reduction of the collection efficiency of the spectrometer whose central wavelength is set on the unshifted fluorescence wavelength.

3. The single photon detection technique

The use of CCD detectors in the so-called single-photon regime for ultrashort and ultraintense laser–plasma X-ray spectroscopy [7,15], is now being considered in particular in sub-PW or PW laser interaction regimes [32]. As it is well known, CCD detectors, while still limited in spatial resolution when compared to X-ray films, offer a number of advantages such as high linearity, dynamic range and quantum efficiency, as well as, with some respects, a higher ease-of-use [33]. When used in the single-photon regime, a CCD detector enables the spectrum of the impinging X-ray radiation to be obtained without any additional dispersing device. This is basically due to the fact that each X-ray photon absorbed in the sensitive layer of the CCD gives rise to a signal (charge) proportional to the photon energy. Due to the large number of pixels in a conventional CCD chip, a few laser shots (ideally one) are required to get an X-ray spectrum in a large energy interval, with a typical resolution well below 10% in the energy range from 1 keV to a few tens of keV.

In principle, a CCD detector enables the X-ray spectrum of a given source to be retrieved, regardless of the X-ray pulse duration, provided that an average of no more than one photon hits each pixel. In practice, due to the charge spreading around neighbouring pixels, the average number of photons per pixel must be typically much less than 1 [34]. This condition can be achieved either by increasing the source-to-detector distance or by placing appropriate filters to attenuate the incident flux on the CCD to the required level [35]. This technique has recently been demonstrated to be effective even at high photon energies, up to around 100 keV [36], making it useful for the study of Bremsstrahlung emission in the ultra-high intensity interaction regime.

The raw image typically consists of a collection of spots (each with its own shape and signal amplitude) corresponding to a single photon interaction with the CCD detector. Images are processed and the charge corresponding to each photon event is measured and converted in incident photon energy through a calibration curve obtained using a set of known X-ray photon energies from both reference radioactive sources and well characterized laser-driven sources [37]. In order to obtain a full spectrum using this technique, a large number of frames are required to reduce the statistical noise. This is typically obtained via acquisition of data from several laser shots. More recently, due to the large area and number of pixels available in commercial CCDs, single shot measurements are becoming possible. The plot of Fig. 1 shows a typical X-ray spectrum obtained from laser irradiation of a 12 μm thick Ti foil at an intensity of 5×10^{17} W/cm^2 using the ILIL fs Ti:Sa laser system which delivers up to 150 mJ in a 65 fs duration pulse. In this case the angle of incidence was 55° and the CCD (Peltier cooled at −5 °C in this

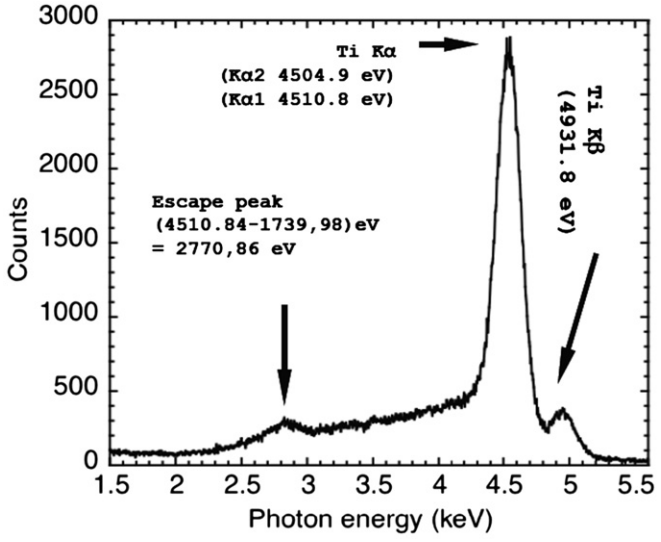

Fig. 1. Spectrum of X-ray emission from a 12 μm thick Ti foil irradiated at an intensity of 5×10^{17} W/cm^2. The spectrum was obtained from accumulation of 30 laser shots (see text for details of the irradiation conditions).

Please cite this article as: L.A. Gizzi, et al., Nucl. Instr. and Meth. A (2010), doi:10.1016/j.nima.2010.04.145

case) detector was looking at the target from the front side, on the horizontal plane, at 10° from the target normal axis.

Clearly visible in the spectrum are the Kα and the Kβ components of X-ray emission generated by fast electron propagation in the substrate of the Ti foil target. Also visible in the spectrum is a small feature at 2.7 keV due to a small number of events in which a Kα photon from an excited atom of the Si substrate of the CCD array escapes from the detector sensitive area. We observe that since this detection technique is based upon a position sensitive device (typically a CCD), it also provides information on the landing position of each X-ray photon. Therefore, depending on the specific experimental set-up, this information can be used to recover the angular distribution of incident X-ray photons or the spatial distribution at the source position. Our energy encoded pin-hole camera (EEPHC) [38], i.e. a pin-hole camera coupled to the CCD detector working in single-hit mode, can therefore be used to obtained full spectral and spatial information on the X-ray source. A detailed account of the instrumental aspects of the technique and the first results obtained with multi-shot operation are given elsewhere [39,40]. Here we focus on the application of this technique to a fast electron transport experiment in single-shot operation typical of large (high energy) laser-systems. In particular we report on recent preliminary results obtained at the Prague Asterix Laser and at the Petawat Laser at RAL.

4. Single-shot, full spectral resolution X-ray imaging

As anticipated above, the same detection principle discussed in the previous sections can be applied to the standard pin-hole camera imaging where the use of small aperture pin-holes enables energy resolved X-ray image reconstruction of a laser plasma X-ray source with high spatial resolution. In fact, provided that the X-ray flux at the image plane is sufficiently low to allow single-photon identification, one can obtain a full, spectrally resolved image by collecting a large number of photons, either by accumulating images over many shots or by collecting many images simultaneously. The final spatial resolution that can be achieved with this new kind of technique is set by the pin-hole aperture (diameter) while the final X-ray contrast of the images is set by the opacity of the substrate in which the pin-hole is drilled. For this reason it is of a fundamental importance to have micron-sized aperture pin-holes on a thick and high Z metal substrate. In the case of interaction experiments with a 10TW laser system mentioned above, a 25 μm thick substrate of Pt was enough to ensure a good contrast, but for the case of a PW laser system, the energy of the produced hot electron is higher and requires higher thickness up to 200 μm of metal like W or Pt. This kind of pin-holes on very thick substrates require a special laser manufacturing technique as described in details in Refs. [41,42]. Another important feature of large laser system is the low repetition rate, of the order of 5–10 laser shot/day. In such circumstances it is not possible to collect the data required for the technique to work taking hundreds of shots. This situation calls for a single-shot approach to this diagnostic technique.

The solution presented here was proposed by the ILIL group as a diagnostic for the experiments of the preparatory phase for the European HIPER project [43]. This set-up enabled us to collect, in a single shot, hundreds of single photon images of the plasma X-ray source. The experimental validation of this single shot diagnostic was carried out in two experiments at the Prague Asterix Laser System (PALS) and at the Vulcan Petawatt Laser (RAL). In both experiments, the technique was successfully used to obtain, for the first time, a fully spectrally resolved image of the X-ray source. Basically the idea is to collect several hundreds of images in a single hit by using a pin-hole array and a large area CCD camera.

4.1. High-energy, long pulse interaction regime

A first use of the energy resolved X-ray imaging working in single shot regime was carried out at the Asterix laser system in the PALS facility in Prague. In this case the 100 J, third harmonic (438 nm) pulses of the iodine laser were focused on target at an intensity of about 2×10^{14} W/cm^2 at normal incidence. The high energy content of the laser pulse was enough to give an high flux of X-rays even in presence of very small aperture pin-holes (about 5 μm). Fig. 2 (left) shows the ensemble of several hundreds of X-ray images obtained in a single shot from interaction with a Ti foil target and with a geometrical magnification factor of about 4.8. The image was filtered with a 6 μm thick Al foil plus 100 μm thick plastic.

The image of Fig. 2 (left) shows the X-ray images at high flux, i.e. away from the single photon counting regime. In this case only the overall X-ray source shape can be recovered as in a normal pin-hole camera while the energy of individual X-ray photons is lost due to the high flux. Starting from images like this, additional filtering is needed to reduce the X-ray flux and enter the single photon counting. Fig. 2 (right) shows the reconstructed X-ray images at the Ti $K_{\alpha,\beta}$ photon energy as obtained in the same condition of Fig. 2 (left) by adding 90 μm of Al. The image has a

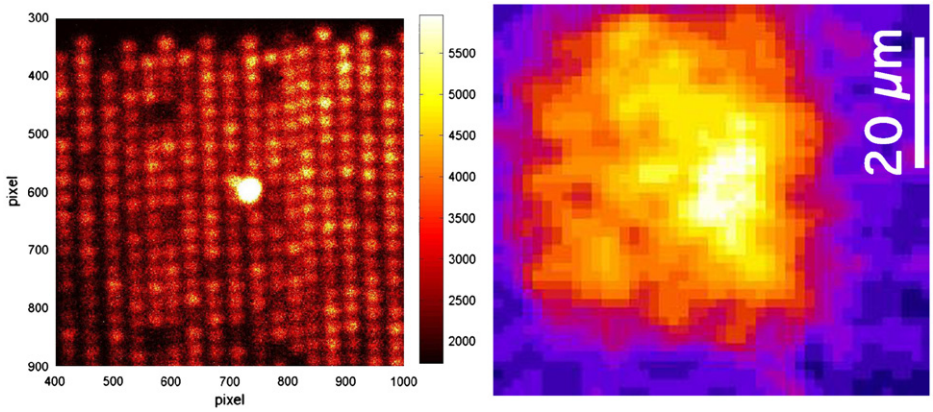

Fig. 2. (Left) Ensemble of several hundreds of X-ray images obtained from interaction of a single-shot of the 100 J laser at PALS with a Ti foil. The image magnification factor was 4.8 and the detector was filtered with a 6 μm thick Al foil plus a 100 μm thick plastic foil. (Right) Full X-ray image after reconstruction and selection of X-ray photons at Ti $K_{\alpha,\beta}$ photon energy. The image was obtained in the same interaction condition of (left), but adding 90 μm of Al to reduce the photon flux at the single photon counting regime.

Please cite this article as: L.A. Gizzi, et al., Nucl. Instr. and Meth. A (2010), doi:10.1016/j.nima.2010.04.145

size of $60 \times 60\,\mu m^2$ in the object plane. In this case the X-ray images are indeed in single photon regime and it was possible to distinguish the energy of single photons on the entire image. The dimension of the source at the Ti $K_{\alpha,\beta}$ photon energy was measured to be about 30 μm. The X-ray spectra were dominated by the $K_{\alpha,\beta}$ fluorescence line of the Ti and no high energy photons were present because of the relatively low laser intensity of $2 \times 10^{14}\,W/cm^2$ and the relatively short laser wavelength that contribute to a small value of $I\lambda^2$ and, therefore, to a low hot electron temperature.

4.2. High energy, short pulse interaction regime.

A second, highly demanding, validation test of the EEPHC working in single shot regime was carried out at the Vulcan laser system of the RAL Laboratory (Didcot, UK). In this case two counter propagating beams were focused on both sides of the same Ti target. The angles of incidence were 20° for the first beam of 60 cm in diameter focused with an f/3 off axis parabola on the front side and 20° for the second beam of 20 cm in diameter focused with an f/3 off axis parabola on the rear side, the angle between the opposed beams was therefore 140°. The nominal focal spot diameter was about 5.5 μm in both cases and the pulse duration was 700 fs FWHM. The total laser energy on both beams was 350 J. Fig. 3 shows a schematic set-up of the experiment with the two beam directions and EEPHC angle of view clearly visible. The CCD used for single photon counting and spectrally resolved imaging was a large area detector consisting of 4700×2200 pixel of $20 \times 20\,\mu m^2$, Peltier cooled at −50 °C and equipped with a 500 μm thick Be window.

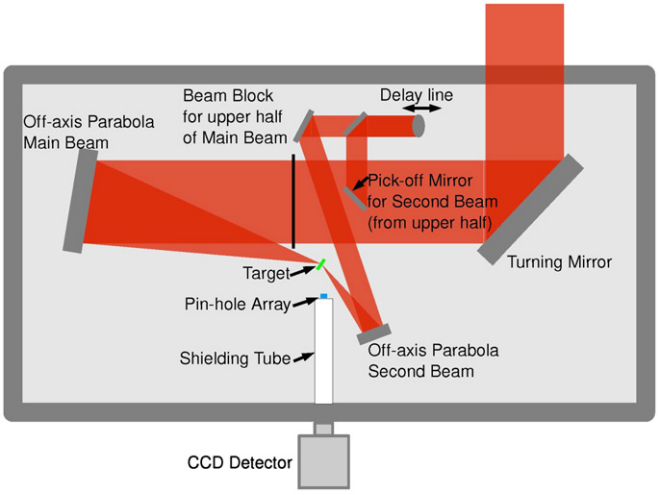

Fig. 3. The utilized set-up for the EEPHC at the Petawat target area, the two beam directions and CCD angle of view are visible.

Because of the ultra-high intensity, high energy electrons are produced in the interaction which, in turn, generate, via Bremsstrahlung from interaction with solids surrounding the target, a large background noise of hard X-rays. Shielding the EEPHC from this noise was a particularly challenging task for the ultra-high intensity interaction regime of the Petawatt Laser. To avoid noise on the CCD, fast electrons must be stopped without generating high energy Bremsstrahlung. This was done by using magnets and plastic stoppers along the line of sight of the detector. Also, to obtain a reasonable X-ray image contrast, a 200 μm Pt substrate was necessary for the custom made PHA. Here we present preliminary results of a shot in which the main beam had an energy of about 340 J. In this shot the focal position of the first beam was moved 200 μm from the best focus to balance the intensity on the target for the two counter-propagating beams.

Fig. 4 (left) shows the full CCD acquired multi-image (shot 090731-003) with the nominal position of each hole superimposed on the image. Fig. 4 (right) shows the final result from superposition of all sub-images in a 140×140 pixel window. The potential of the technique is clearly visible from the images of Fig. 5 which shows the raw X-ray spectrum where the TiKα and CuKα emission line are superimposed on a broad high energy Bremsstrahlung emission. The explanation of the physical mechanisms responsible for these observations is very complex and beyond the scope of this work. However, a detailed analysis of these results shows that very high energy photons originate from a small central region, most likely corresponding to the region directly heated by the laser pulse. In contrast, X-ray emission in the 4–10 keV region where, in our case, most of the fluorescence emission (we recall that the TiKα is 4.5 keV), originates from peripheral regions, away from the laser irradiated region. This is most likely due to the combined effect of fast electrons and self-generated magnetic fields that give rise to the so-called

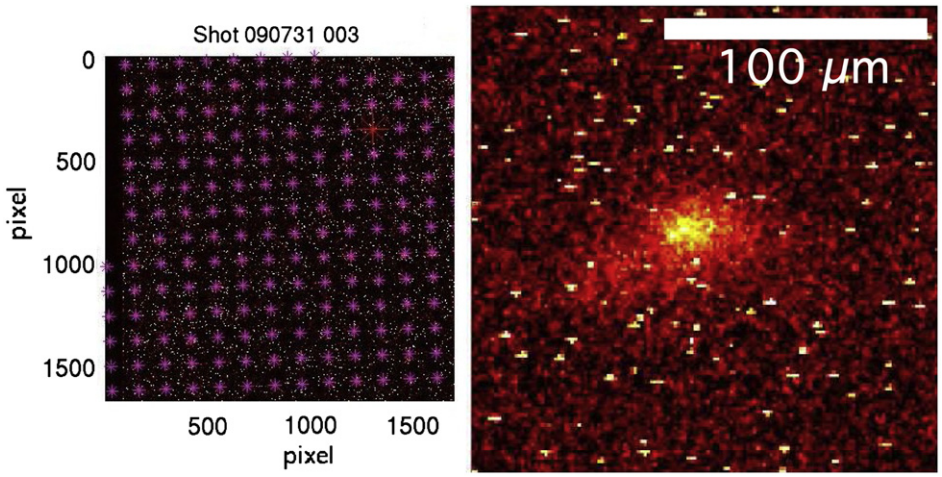

Fig. 4. (Left) Full CCD image (shot 090731-003) showing individual X-ray photons from each image. Superimposed on the image are also visible the reference positions of each pin-hole of the array. (Right) Raw image showing the final result from superposition of all sub-images; the image corresponds to a $180 \times 180\,\mu m^2$ wide region in the plasma plane.

Please cite this article as: L.A. Gizzi, et al., Nucl. Instr. and Meth. A (2010), doi:10.1016/j.nima.2010.04.145

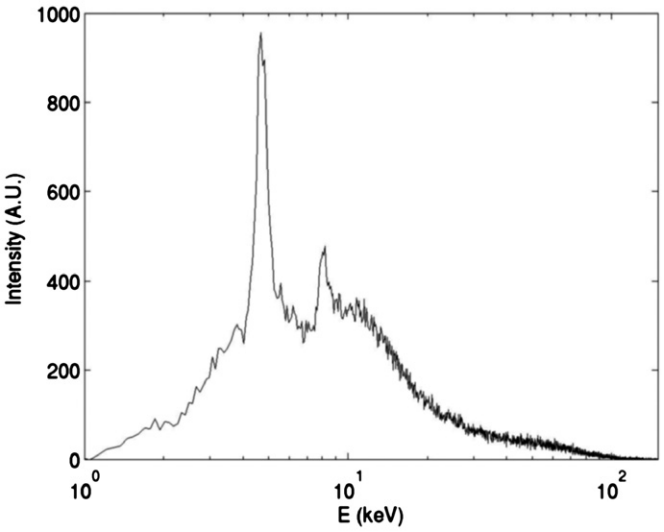

Fig. 5. Raw X-ray spectra where the TiKα and CuKα emission lines are clearly visible over a broad high energy bremsstrahlung emission.

fountain effect, in which fast electrons escaping from the target are pulled back onto the target by the action of magnetic fields and penetrate in the cold target substrates producing X-ray fluorescence.

These results show, to our knowledge for the first time, that the X-ray single photon counting mode can be combined with a pin-hole camera concept, extended to a pin-hole camera array configuration in a new Energy Encoded Pin Hole Camera (EEPHC) concept. Here we have shown an example in which this EEPHC was used to acquire information on the different region characterized by different contributions to the X-ray emission.

5. Summary and conclusions

In summary, we discussed the main issues concerning experimental investigation of fast-electron transport in solids irradiated at ultra-high intensity using high-power, femtosecond laser pulses. Limitations of basic spectroscopic diagnostic techniques based upon well established Bragg crystal spectrometers can be overcome by a novel experimental technique, the Energy Encoded Pin Hole Camera (EEPHC), capable of full imaging with spectral resolution of the X-ray emission from laser irradiated targets. The technique, based upon a pin-hole camera equipped with a pin-hole array and a CCD detector operating in the so-called single-photon regime, allows the image in any given spectral window in the keV range to be obtained, provided the X-ray response of the CCD has been previously characterized. Preliminary results were presented from validation experiments of the EEPHC for single shot experiments. These results show for the first time an X-ray image of laser interaction at an intensity exceeding 10^{19} W/cm^2 from which the different X-ray emission regions dominated either by direct laser irradiation or by X-ray fluorescence due to fast electron energy deposition can be identified.

Acknowledgements

This work was carried out in the framework of the HiPER Project. Access to the Vulcan Petawatt Laser and to the Prague Asterix Laser were supported by the LASERLAB (grant agreement no 228334). We wish to acknowledge the TAP and PALS laser and target area crew for their invaluable support. We acknowledge additional financial support by the ESF-COST Action MP0601, by the MIUR-FIRB project "SPARX", by the MIUR-PRIN-2007 project "Studio della generazione di elettroni veloci nell'interazione laser–plasma ad alta intensità". The present work is part of the "High Field Photonics" CNR Research Unit.

References

[1] M. Perry, G. Morou, Science 264 (1994) 917.
[2] D. Stickland, G. Mourou, Opt. Commun. 56 (1985) 219.
[3] M.M. Murnane, H.C. Kapteyn, R.W. Falcone, Phys. Rev. Lett. 62 (1989) 155.
[4] M. Tabak, J. Hammer, M. Glinsky, W.L. Kruer, S.C. Wilks, J. Woodworth E.M. Campbell, M.D. Perry, Phys. Plasmas 1 (1994) 1626.
[5] S. Atzeni, J.R. Davies, L. Hallo, J.J. Honrubia, P.H. Maire, M. Olazabal-Loumé, J.L. Fuegeas, X. Rybeire, A. Schiavi, G. Schurtz, J. Breil, Ph. Nicolaï, Nuclear Fusion 49 (2009) 055008 (7pp).
[6] A. Rousse, P. Audebert, J.P. Geindre, F. Fallies, J.C. Gauthier, A. Mysyrowicz, G. Grillon, A. Antonetti, Phys. Rev. E 50 (1994) 2200.
[7] L.A. Gizzi, A. Giulietti, D. Giulietti, P. Audebert, S. Bastiani, J.P. Geindre, A. Mysyrowicz, Phys. Rev. Lett. 76 (1996) 2278.
[8] L.A. Gizzi, A. Giulietti, D. Giulietti, P. Köster, L. Labate, T. Levato, F. Zamponi, A. Lübcke, T. Kämpfer, I. Uschmann, E. Förster, A. Antonicci, D. Batani, Plasma Phys. Controlled Fusion 49 (2007) B211.
[9] R.A. Snavely, M.H. Key, S.P. Hatchett, T.E. Cowan, M. Roth, T.W. Phillips M.A. Stoyer, E.A. Henry, T.C. Sangster, M.S. Singh, S.C. Wilks, A. Mackinnon A. Offenberger, D.M. Pennington, K. Yasuike, A.B. Langdon, B.F. lasinski, J. Johnson, M.D. Perry, E.M. Campbell, Phys. Rev. Lett. 85 (2000) 2945.
[10] H. Alfven, Phys. Rev. E 55 (1939) 425.
[11] A.R. Bell, J.R. Davies, S.M. Guerin, Plasma Phys. Controlled Fusion 39 (1997) 653.
[12] S.C. Wilks, W.L. Kruer, IEEE J. Quantum Electron. 33 (1997) 1954.
[13] P. Gibbon, E. Förster, Plasma Phys. Controlled Fusion 38 (1996) 769.
[14] F. Brunel, Phys. Rev. Lett. 59 (1987) 52.
[15] L. Labate, M. Galimberti, A. Giulietti, D. Giulietti, P. Köster, P. Tomassini, L.A. Gizzi, Appl. Phys. B 86 (2006) 229.
[16] J. Limpouch, O. Klimo, V. Bína, S. Kawata, Laser Particle Beams 22 (2004) 147.
[17] L.M. Chen, P. Forget, S. Fourmaux, J.C. Kieffer, A. Krol, C.C. Chamberlain, B.X. Hou, J. Nees, G. Mourou, Phys. Plasmas 11 (2004) 4439.
[18] C. Reich, P. Gibbon, I. Uschmann, E. Förster, Phys. Rev. Lett. 84 (2000) 4846.
[19] B. Soom, H. Chen, Y. Fisher, D.D. Meyerhofer, J. Appl. Phys. 74 (1993) 5372.
[20] U. Teubner, I. Uschmann, P. Gibbon, D. Altenbernd, E. Förster, T. Feurer, W. Theobald, R. Sauerbrey, G. Hirst, M.H. Key, J. Lister, D. Neely, Phys. Rev. E 54 (1996) 4167.
[21] G. Pretzler, F. Brandl, J. Stein, E. Fill, J. Kuba, Appl. Phys. Lett. 82 (2003) 3623.
[22] C. Reich, I. Uschmann, S. Düsterer, A. Lübcke, H. Schwoerer, R. Sauerbrey, E. Förster, Phys. Rev. E 68 (2003) 056408.
[23] T. Feurer, A. Morak, I. Uschmann, C. Ziener, H. Schwoerer, C. Reich, P. Gibbon, E. Förster, R. Sauerbrey, Phys. Rev. E 65 (2001) 016412.
[24] C. Ziener, I. Uschmann, G. Stobawra, C. Reich, P. Gibbon, T. Feurer, A. Morak, S. Düstere, H. Schwoerer, E. Förster, R. Sauerbrey, Phys. Rev. E 65 (2002) 066411.
[25] H. Nishimura, T. Kawamura, R. Matsui, Y. Ochi, S. Okihara, S. Sakabe, F. Kolke, T. Johzaki, H. Nagatomo, K. Mima, I. Uschmann, E. Förster, J. Quantit. Spectr. Radiat. Transfer 81 (2003) 327.
[26] D. Batani, Laser Particle Beams 20 (2002) 321.
[27] F. Ewald, H. Schwoerer, R. Sauerbrey, Europhys. Lett. 60 (2002) 710.
[28] Y. Sentoku, K. Mima, T. Taguchi, S. Myiamoto, Y. Kishimoto, Phys. Plasmas 5 (1998) 4366.
[29] R. Rosch, J.Y. Boutin, J.P. le Breton, D. Gontier, J.P. Jadaud, C. Reverdin, G. SoulliŽ, G. Lidove, R. Maroni, Rev. Sci. Instrum. 78 (2007) 033704.
[30] R.B. Stephens, R.A. Snavely, Y. Aglitskiy, F. Amiranoff, C. Andersen, D. Batani, S.D. Baton, T. Cowan, R.R. Freeman, T. Hall, S.P. Hatchett, J.M. Hill, M.H. Key, J.A. King, J.A. Koch, M. Koenig, A.J. MacKinnon, K.L. Lancaster, E. Martinolli, P. Norreys, E. Perelli-Cippo, M. Rabec Le Gloahec, C. Rousseaux, J.J. Santos F. Scianitti, Phys. Rev. E 69 (2004) 066414.
[31] C. Stoeckl, W. Theobald, T.C. Sangster, M.H. Key, P. Patel, B.B. Zhang, R. Clarke, S. Karsch, P. Norreys, Rev. Sci. Instrum. 75 (2004) 3705.
[32] H. Park, N. Izumi, M.H. Key, J.A. Koch, O.L. Landen, P.K. Patel, T.W. Phillips, B.B. Zhang, Rev. Sci. Instrum. 75 (2004) 4048.
[33] S.M. Gruner, M.W. Tate, E.F. Eikenberry, Rev. Sci. Instrum. 73 (2002) 2815.
[34] G.W. Fraser, X-ray Detectors in Astronomy, Cambridge University Press, Cambridge, 1989.
[35] L. Labate, T. Levato, M. Galimberti, A. Giulietti, D. Giulietti, M. Sanna, C. Traino, M. Lazzeri, L.A. Gizzi, Nucl. Instr. and Meth. Phys. Res. A 594 (2008) 278.
[36] T. Levato, L. Labate, M. Galimberti, A. Giulietti, D. Giulietti, L.A. Gizzi, Nucl. Instr. and Meth. Phys. Res. A 592 (2008) 346.
[37] L. Labate, M. Galimberti, A. Giulietti, D. Giulietti, L.A. Gizzi, P. Tomassini, G. Di Cocco, Nucl. Instr. and Meth. Phys. Res. A 495 (2001) 148.

Please cite this article as: L.A. Gizzi, et al., Nucl. Instr. and Meth. A (2010), doi:10.1016/j.nima.2010.04.145

[38] L. Labate, E. Förster, A. Giulietti, D. Giulietti, S. Höfer, T. Kämpfer, P. Köster, M. Kozlova, T. Levato, R. Lötzsch, A. Lübcke, T. Mocek, J. Polan, B. Rus, I. Uschmann, F. Zamponi, L.A. Gizzi, Laser Particle Beams 27 (2009) 643.
[39] L. Labate, A. Giulietti, D. Giulietti, P. Köster, T. Levato, L.A. Gizzi, F. Zamponi, A. Lübcke, T. Kämpfer, I. Uschmann, E. Förster, Rev. Sci. Instrum. 78 (2007) 103506.
[40] L.A. Gizzi, A. Giulietti, D. Giulietti, P. Köster, L. Labate, T. Levato, F. Zamponi, A. Lübcke, T. Kämpfer, I. Uschmann, E. Förster, A. Antonicci, D. Batani, Plasma Phys. Controlled Fusion 49 (2007) B221.
[41] T. Levato, L. Labate, N.C. Pathak, C. Cecchetti, P. Koester, E. Di Fabrizio, P. Delogu, A. Giulietti, D. Giulietti, L.A. Gizzi, Nucl. Instr. and Meth. Phys. Res. A Proceedings, this issue.
[42] T. Levato, N.C. Pathak, C.A. Cecchetti, O. Ciricosta, P. Koester, L. Labate, A. Giulietti, D. Giulietti, F. De Angelis, E. Di Fabrizio, P. Delogu, L.A. Gizzi, AIP Conference Proceedings Series, February 2, 2010, vol. 1209, pp. 59–62, doi:10.1063/1.3326308.
[43] 〈http://www.hiperlaser.org〉.

Please cite this article as: L.A. Gizzi, et al., Nucl. Instr. and Meth. A (2010), doi:10.1016/j.nima.2010.04.145